CWJ

4:45 pm–6:30 pm
Room: 101B

Novel Biomedical Imaging and Detection

Gregory Faris, SRI International, USA, Presider

CWJ1 **4:45 pm**

Investigation of Tumor Recognition by Terahertz Dark-field Imaging

T. Löffler, T. Bauer, K.J. Siebert, and H.G. Roskos, Physikalisches Institut, Johann Wolfgang Goethe—Universität Frankfurt, Robert-Mayer-Straße 22-4, D-60054 Frankfurt (Main), Germany

A. Fitzgerald, Centre of Medical Imaging Research, University of Leeds, Great George Street, Leeds LS1 3EX, England

S. Czasch, Institut für Veterinär-Pathologie, Universität Gießen, Frankfurter Str. 96, D-35392 Gießen, Germany

Dark-field imaging deals with contrast enhancement by the detection of that part of the radiation which is deflected out of the beam-propagation direction by either diffraction or scattering in the sample, and requires blocking of the ballistic part of the radiation.

THz pulses are generated at a repetition rate of 1 kHz via optical rectification, focused onto the sample with a cone angle of 10° and detected electro-optically after transmission through the sample. As the radiation from the sample is collected within a much larger cone angle of 45°, a large amount of radiation diffracted and scattered within the sample is detected in addition to the ballistic radiation. In order to perform dark-field imaging, the latter is blocked by a metal beam stop.[1]

We performed measurements on a 3-mm-thick archived (formalin-fixed, alcohol-dehydrated, embedded-in-paraffin) canine skin tissue sample containing a mast cell tumor in bright-field and in dark-field geometry. 2176 pixels are imaged in a total measurement time of 3 hours per image. Figure 1(a) exhibits a photograph of the scanned area of the sample. Areas of fat, skin with hairs, connective tissue and the tumor are indicated.

Images of the total loss obtained from a measurement without beam stop are depicted in Fig. 1(b) for 0.6 THz and in Fig. 1(c) for 2 THz. The images in Figs. 1(d) and (e) display the deflection loss (the ratio of the power deflected relative to the power transmitted through pure paraffin) for 0.6 THz and 2.0 THz. In the tumor region, the deflection loss at 2.0 THz is exceedingly small (approaching the noise level). In order to correct for the influence of absorption in the dark-field images, we define a new quantity, the deflection coefficient, as the ratio of the deflection loss to the absorption loss. This quantity is equivalent to the relative part of the power that would be deflected from a non-absorbing or infinitely thin sample. The resulting images are depicted in Figs. 1(f) and 1(g). The data taken at 2.0 THz show that the tumor region is not a strong deflector quite in contrast to the boundaries between different tissue types and the area of the skin with hairs. Comparison with the data taken at 0.6 THz suggests that diffraction is dominant at boundaries, while scattering dominates in the region of skin with hairs.

In Fig. 1(f) we demonstrate that the tumor region may be identified by combining criteria for the total loss and the deflection loss at 2 THz as specified in the figure.

In summary we believe, that THz dark-field imaging, which allows enhancing of imaging contrast especially at tissue boundaties, holds promise for the clinical distinction between benign and malignant tumors, as this is usually based on differences in the structure of the tumor boundary. For in-vivo applications a reflection geometry, like in Ref. [2] has to be introduced.

This work was supported by EU project TERAVISION under contract no. IST-1999-10154 and by GSI contract no. OF-ROS.

1. T. Löffler, T. Bauer, K.J. Siebert, H.G. Roskos, A. Fitzgerald, and S. Czasch, "Terahertz dark-field imaging of biomedical tissue" submitted to Optics Express.
2. R.M. Woodward, B. Cole, V.P. Wallance, D.D. Arnone, R. Pye, E.H. Linfield, M. Pepper, and A.G. Davies, CLEO 2001, CWE4, pp. 329.

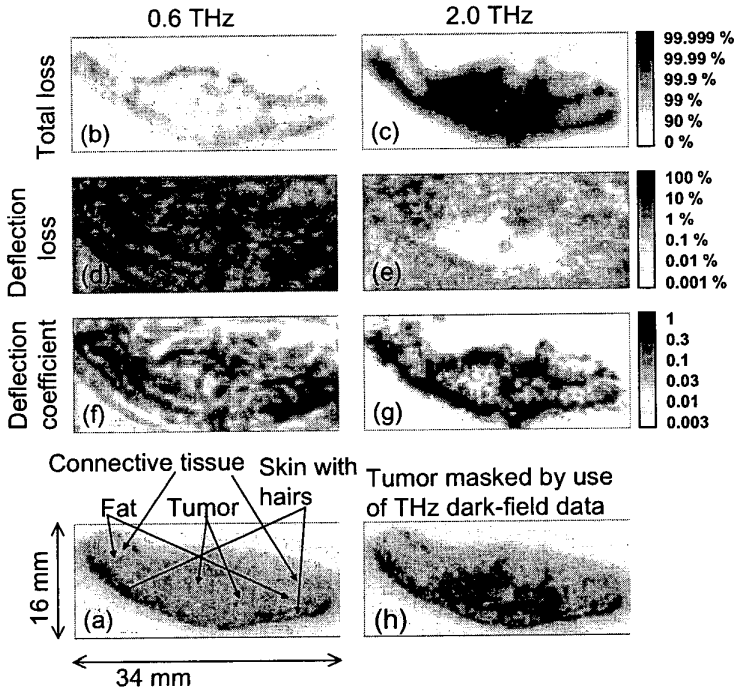

CWJ1 Fig. 1. (a) Optical image of the sample; (b) and (c): Total loss in transmission, (d) and (e): Loss induced by deflection; (f) and (g): Deflection coefficient. (h) Optical image of the sample overlapped with a dark mask generated at areas where deflection loss is smaller than 0.05% and the total loss is larger than 95%.

CWJ2 **5:00 pm**

Compact and Cost-effective Continuous Wave THz Imaging System

T. Kleine-Ostmann, P. Knobloch, M. Koch, Institut für Hochfrequenztechnik, Technische Universität Braunschweig, D-38106 Braunschweig, Germany, Email: martin.koch@tu-bs.de

S. Hoffmann, M. Hofmann, Institut für Werkstoffe der Elektrotechnik, Ruhr-Universität-Bochum, D-44780 Bochum, Germany

G. Hein, and K. Pierz, Physikalisch-Technische Bundesanstalt, Bundesallee 100, D-38116 Braunschweig, Germany

Imaging in the spectral range between a few hundred GHz and several THz holds great potential for a variety of applications including material

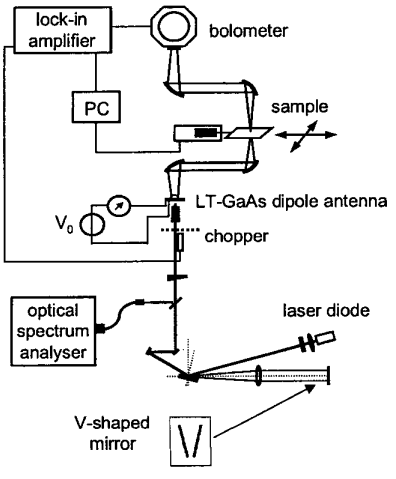

CWJ2 Fig. 1. Setup of the continuous-wave THz imaging system including the two-mode external cavity laser diode, a LT-GaAs photomixer and a bolometer.

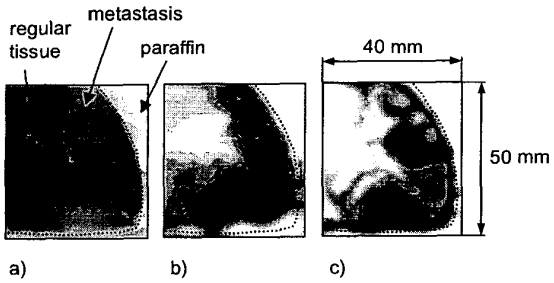

CWJ2 Fig. 2. Images of a liver sample with tumors: a) optical image, b) cw THz transmission image at 230 GHz, c) THz transmission image for a frequency window from 0.2 to 0.5 THz obtained with pulsed radiation.

sciences and medical diagnosis. During the last years THz technology has been developed to a stage where first commercial systems are available. Yet, the THz imaging systems developed so far all work in the time-domain using THz pulses. Hence, they rely on expensive and bulky femtosecond lasers as a key component.

Here, we present the first continuous-wave THz imaging system. CW THz radiation is generated via photomixing in a LT-GaAs dipole antenna.[1] As optical pump source we use a recently developed external cavity two-color laser,[2,3] which is quite compact and inexpensive. The cw system is superior to time-domain systems if high spectral resolution and high spectral power density are called for.

The system setup is shown in Fig. 1. Its pump source is a semiconductor laser diode in a Fourier-transform external cavity which disperses the different wavelengths of the gain spectrum to different positions on the end mirror. Wavelength selection and tuning can be achieved by using an aperture right in front of the end mirror. The aperture might be a mechanical slit or a liquid crystal array (LCA); the later giving purely electronic tunability. If the LCA is adjusted so that two wavelengths experience a properly balanced feedback the laser runs simultaneously on both.[2] Yet, instead of the LCA we use here a V-shaped mirror for simplicity. The frequency spacing of the two laser modes can then be adjusted by moving the V-mirror vertically. For the measurements presented below it is set to 230 GHz which corresponds to the resonance frequency of our dipole antenna onto which the laser emission is focused (total power 29 mW). For detection we use a standard bolometer. To obtain an image the sample is scanned through an intermediate focus and the transmitted THz power is detected pixel by pixel using the lock-in technique.

The cw imaging setup is used to study several bio-medical samples that have undergone the standard procedure for histo-pathological investigation.[4] Fig. 2a shows an *optical* image of a sample from a human liver with several tumors. The size of the entire sample is 50 × 40 × 4 mm. The cancerous areas appear somewhat brighter than the regular tissue. Fig. 2b shows a *cw THz* image in which the tumors appear as dark patches of reduced transmission and are clearly distinguishable from regular tissue. The level of detail is not as good as that of a previously measured transmission image (Fig. 2c) using pulsed THz radiation which we show here for comparison. This is simply because the cw frequency of 230 GHz is located at the lower end of the integration interval from 0.2 to 0.5 THz used for the pulsed image leading to a smaller spatial resolution. The question whether the differences in transmission between regular and cancerous tissue are due to a different density or a different chemical composition is currently addressed.

References

1. E.R. Brown, K.A. McIntosh, K.B. Nichols, C.L. Dennis, Appl. Phys. Lett. 66, 285 (1995).
2. J. Struckmeier, A. Euteneuer, B. Smarsly, M. Breede, M. Born, M. Hofmann, L. Hildebrand and J. Sacher, Optics Letters 24, 1753 (1999).
3. P. Gu, F. Chang, M. Tani, K. Sakai, C.-L. Pan, J. Appl. Phys. 38, L 1246 (1999).
4. P. Knobloch, K. Schmalstieg, M. Koch, E. Rehberg, F. Vauti, and K. Donhuijsen, Proceedings of the European Conferences on Biomedical Optics, June 2001, Munich, Germany.

CWJ3 **5:15 pm**

Mid-Infrared Laser Delivery into a Precise Tissue Area Using a Smart, Tissue-activated Optical Fiber Probe

Ilko K. Ilev, Ronald W. Waynant, US Food and Drug Administration, Center for Devices and Radiological Health, HFZ-134, Rockville, MD 20857, Email: Ilko_Ilev@eob.cdrh.fda.gov, Ron_Waynant@eob.cdrh.fda.gov,

Mary Reiter, Department of Biomedical Engineering, Marquette University, Milwaukee, WI 53201, Email: mary.reiter@marquette.edu

The mid-infrared (mid-IR) spectral region is of great importance in medical research and instrumentation since the most identifiable molecules have specific IR absorption and radiation features that depend upon their exact chemical composition.[1] With respect to mid-IR optical fiber (OF) based laser delivery systems that are used in biomedicine, the research efforts are focused on the investigation of low-loss IR fiber systems that provide an efficient and broadband delivery of powerful mid-IR laser radiation including from Er:YAG, free-electron and CO_2 lasers. Here, we present a novel all-optical-fiber system for mid-IR laser delivery into a precise tissue area using a direct laser-to-taper coupling and a smart, tissue-activated delivery OF with an angle-shaped tip.

A principal optical arrangement of the suggested all-optical-fiber laser delivery system is shown in Fig. 1. It is a simple single-fiber delivery technique based on the principle of frustrated-total-internal-reflectance caused by the refractive-index change of the surrounding medium and the occurrence of an evanescent field at the fiber-tissue boundary.[2] The all-optical-fiber delivery system includes two specific OF elements: a lens-free, laser-to-fiber coupler, and a delivery OF. In our experiment, instead of a conventional lens-based laser-to-fiber coupler, we utilize an uncoated glass hollow taper as a laser-to-fiber coupler. It is a funnel-shaped taper based upon the grazing-incidence effect.[3,4] The laser emission is launched directly into the taper and then into the delivery OF. The OF is a key element in the system, it performs several functions: (1) it delivers the forward laser emission to the tissue to be treated, and (2) it provides a regime of evanescent-wave delivery because we use a specially shaped OF tip with a 45° angled profile (see Fig. 1b). When the OF tip is not touching the tissue area, the laser emission is backreflected at the an-

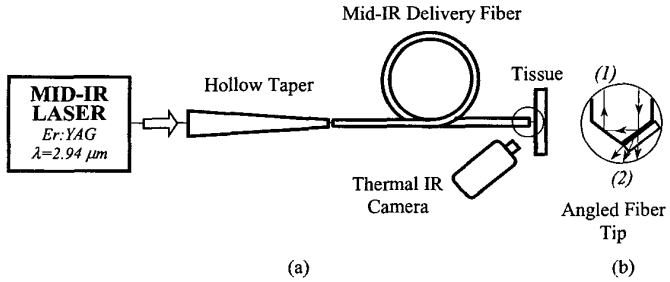

CWJ3 Fig. 1. Experimental setup (a) of the all-optical-fiber system for mid-IR laser delivery into a precise tissue area using a specially shaped OF tip (b) that provides either a total-internal-reflectance (ray 1) or a frustrated-total-internal-reflectance (rays 2) regime depending on the refractive-index of the surrounding medium.